Biomatter 3:4, e25633; October/November/December 2013; © 2013 Landes Bioscience

Mechanical and biocompatible characterization of a cross-linked collagen-hyaluronic acid wound dressing

James F Kirk[1], Gregg Ritter[1], Isaac Finger[1], Dhyana Sankar[1], Joseph D Reddy[1], James D Talton[1], Chandra Nataraj[2], Sonoko Narisawa[3], José Luis Millán[3], and Ronald R Cobb[1,*]

[1]Research and Development Department; Nanotherapeutics, Inc.; Alachua, FL USA; [2]MLM Biologics; Gainesville, FL USA; [3]Sanford-Burnham Medical Research Institute; La Jolla, CA USA

Keywords: collagen sponge, hyaluronic acid, cross-linking, histology, wound repair

Collagen scaffolds have been widely employed as a dermal equivalent to induce fibroblast infiltrations and dermal regeneration in the treatment of chronic wounds and diabetic foot ulcers. Cross-linking methods have been developed to address the disadvantages of the rapid degradation associated with collagen-based scaffolds. To eliminate the potential drawbacks associated with glutaraldehyde cross-linking, methods using a water soluble carbodiimide have been developed. In the present study, the glycosaminoglycan (GAG) hyaluronic acid (HA), was covalently attached to an equine tendon derived collagen scaffold using 1-ethyl-3-(3-dimethyl aminopropyl) carbodiimide (EDC) to create ntSPONGE™. The HA was shown to be homogeneously distributed throughout the collagen matrix. In vitro analyses of the scaffold indicated that the cross-linking enhanced the biological stability by decreasing the enzymatic degradation and increasing the thermal denaturation temperature. The material was shown to support the attachment and proliferation of mouse L929 fibroblast cells. In addition, the cross-linking decreased the resorption rate of the collagen as measured in an intramuscular implant model in rabbits. The material was also shown to be biocompatible in a variety of in vitro and in vivo assays. These results indicate that this cross-linked collagen-HA scaffold, ntSPONGE™, has the potential for use in chronic wound healing.

Introduction

Biological scaffold materials composed of extracellular matrix (ECM) have been shown to facilitate the reconstruction and remodeling of numerous different tissues. Autologous tissue has limited availability and the retrieval of sufficient material may result in additional donor site morbidity.[1] Intrinsic drawbacks of autologous materials have motivated research to identify new biological scaffold materials. These scaffold materials are derived from numerous different tissues including blood vessels,[2–5] tendons and ligaments,[6,7] muscle,[8] skin,[9] small intestines,[10–12] and urinary bladders.[13–15] The ECM materials consists of a complex mixture of molecules that mediate structural and biological properties that entice cells to attach, leading to rapid repopulation and remodeling of the scaffold. Typically, these ECM materials are biodegradable unless processed in such a manner that irreversibly cross-links the resident molecules. The composition and structure of these ECM materials, as well as their in vivo degradability, has marked effects on the host response and remodeling that determine the eventual clinical outcome.

The use of artificial and natural tissue substitute matrices for repair and replacement of tissue defects is a common treatment for many conditions.[16] Biological implants are often the materials of choice in complicated surgical procedures or procedures where there is bacterial contamination or risk of contamination.[17] Collagen is a commonly used biomaterial and has found diverse applications in the biomedical field due to its excellent biocompatibility and controllable biodegradation.[18–20] However, the fast degradation rate of non-treated collagen can't match the demand of in vivo applications in many cases and has been one of the crucial factors that limit the use of this material. Cross-linking of the collagen scaffold is an effective way to slow the biodegradation rate.[21,22] Therefore, the cross-linking treatment of collagen has become one of the most important issues for the clinical use of a collagen scaffold.

Cross-linking of collagen is frequently used to maintain the matrix function during the desired usage of the scaffold.[23] Glutaraldehyde is the most common and convenient cross-linking agent used in the treatment of collagen. It can enhance the biological stability of the collagen matrix by bridging amine groups between two adjacent polypeptide chains. This cross-linking can

*Correspondence to: Ronald R Cobb; Email: rcobb@nanotherapeutics.com
Submitted: 01/12/13; Revised: 06/24/13; Accepted: 07/04/13
Citation: Kirk JF, Ritter G, Finger I, Sankar D, Reddy JD, Talton JD, Nataraj C, Narisawa S, Millán JL, Cobb RR. Mechanical and biocompatible characterization of a cross-linked collagen-hyaluronic acid wound dressing. Biomatter 2013; 3:e25633; http://dx.doi.org/10.4161/biom.25633

Table 1. Criteria for evaluating cytotoxicity

Grade	Reactivity	Conditions of culture
0	None	Discreet intracytoplasmic granules; no cell lysis
1	Slight	Not more than 20% of the cells are round, loosely attached, and without intracytoplasmic granules; occasional lysed cells are present
2	Mild	Not more than 50% of the cells are round and devoid of intracytoplasmic granules; no extensive cell lysis and empty areas between cells
3	Moderate	Not more than 70% of the cell layers contain rounded cells and/or lysed
4	Severe	Nearly complete destruction of the cell layers

Table 2. Cytotoxicity of ntSPONGE™

Test article/treatment	24 h	48 h	72 h
Test article 1:2 dilution	0/0/0	1/1/1	1/1/1
Test article 1:4 dilution	0/0/0	0/0/0	0/0/0
Test article 1:8 dilution	0/0/0	0/0/0	0/0/0
Test article 1:16 dilution	0/0/0	0/0/0	0/0/0
Positive control	4/4/4	4/4/4	4/4/4
Intermediate control	2/2/2	2/2/2	2/2/2
Negative control	0/0/0	0/0/0	0/0/0
Cell control	0/0/0	0/0/0	0/0/0

Summary of cytotoxicity scores for ntSPONGE™ and empty syringe assembly extracts in L-929 cell culture.

also suppress the immunogenicity of the implant.[24] The increase in stability of the matrix comes with some drawbacks such as potential over cross-linking and cytotoxicity.[25–27] Therefore, several alternative cross-linking agents such as 1-ethyl-3-(3-dimethyl aminopropyl)carbodiimide (EDC), polyepoxidic and polyglycidyl have been developed.[23,28,29] Cross-linking of collagen using the water soluble carbodiimide EDC has been shown to result in non-cytotoxic and biocompatible materials.[30,31]

Collagenous biomaterials have found substantial usage for the repair and regeneration of tissues like bone, tendon, skin and cartilage.[19,20,32] For the application of collagen-glycosaminoglycans (GAGs) matrices in tissue engineering, various parameters have to be controlled. These include amount, bioavailability, and location of the GAGs within the matrix. The degradation of the collagen-GAGs matrices must also be taken into consideration since the resorption rate in vivo determines, to a substantial extent, the ability of the scaffold to improve or restore tissue function.

Hyaluronic acid (HA) is an important component of the extracellular matrix and has been used as a viscoelastic biomaterial for medical purposes, in cosmetics and as a drug delivery system. HA is a mucopolysaccharide found in various tissues and its immunoneutrality makes it an excellent building block for biomaterials to be employed for tissue engineering. HA exists in high concentrations in fetal skin development, is involved in cell migration and differentiation and is the first macromolecule to appear in the extracellular matrx during wound healing.[33,34] For the design of ntSPONGE™ hyaluronic acid was selected as the most suitable GAG for inclusion in the wound dressing matrix. HA is a natural component of skin and many connective tissues and known to be a component of healing skin.[35–37] HA is also a hydrogel with inherent absorption properties that are desirable in the wound healing environment for retaining moisture and managing fluid exudate. The combination of HA and collagen fibers has shown advantages such as enhancement of cell migration and division compared with either material alone.[18] There are wound dressings and treatments (HYAFF®, Fidia; Hyalofill®, Convatec; Hyalomatrix®, Misonix) based on hyaluronic acid currently on the market today, but not in the proposed combination.

EDC has been shown to modify side-groups on proteins to make them reactive with other side groups and to mediate the ester bond formation between the hydroxyl and carboxyl groups of HA. Therefore, it has been of widespread use in cross-linking of HA, collagen, and gelatin.[38] Based on these functions, we utilized EDC in the cross-linking of collagen and HA by the amide and ester bond formation of the side groups.

Collagen based products are highly absorptive and maintain a moist wound environment, which promotes autolytic debridement and pain reduction. In the present study, we present an in depth characterization of the biochemical makeup of a novel collagen based sponge wound dressing, ntSPONGE™. The results of the studies presented herein indicate that the novel cross-linked collagen sponge (ntSPONGE™) would be safe and biocompatible for human usage.

Results

Cytotoxicity. A cultured mouse fibroblast cell line (L929 cells) was used to measure the potential cytotoxic effects of the ntSPONGE material. A score of 3 and above is considered cytotoxic and a score of 0–2 was considered non-toxic (**Table 1**). As shown in **Table 2**, ntSPONGE™ material did not induce a substantial cytotoxic response as measured throughout the experiment, in a similar manner as that of the negative control. Cultures exposed to the positive control ($CdCl_2$) exhibited a toxic response while cultures exposed to the black rubber induced a mild toxic response.

Genotoxicity/Mutagenicity. Table 3A summarizes the reversion rates (colony count data) for the strains of *S. typhimurium* in the presence or absence of ntSPONGE™ extract or 2-AA, a known mutagen requiring metabolic transformation (S9). **Table 3B** summarizes the reversion rates in the presence or absence of ntSPONGE™ extract or a known direct-acting mutagen in the absence of S9. A 2-fold or greater increase in reversion rate

Table 3A. Genotoxicity/mutagenicity of ntSPONGE™

Strain	ntSPONGE™ NS extract	NS	ntSPONGE™ DMSO extract	DMSO	2-AA
TA97a	138.3	152	141.3	136.3	2163
TA98	33.7	32.7	32.7	33.3	1933.3
TA100	104.7	118	104.7	102	1122.3
TA1535	18	13.7	12.7	15	140
WP2-uvrA-	19.3	20	16	21.3	256.7

Average colony counts (n = 3) for the strains of *S. typhimurium* used in the Ames Assay in the presence or absence of ntSPONGE™ extract or 2-AA with S9 activation.

Table 3B. Genotoxicity/mutagenicity of ntSPONGE™

Strain	ntSPONGE™ NS extract	NS	ntSPONGE™ DMSO extract	DMSO	Mutagen
TA97a	90.7	112.3	108.7	94	ICR-191 (1045.7)
TA98	31	31	29.3	25	2-NF (1055.7)
TA100	116.7	115	95.7	115.7	Na Azide (901.7)
TA1535	15.7	18.7	11.7	16	Na Azide (364.7)
WP2-uvrA-	19.7	23.7	21.7	19.3	MNNG (108)

Average colony counts (n = 3) for the strains of *S. typhimurium* used in the Ames Assay in the presence or absence of ntSPONGE™ extract or a direct-acting without S9 activation.

Table 4. Mouse lymphoma assay

Treatment	Device extract NS	Device extract DMSO	Vehicle control NS	Vehicle control DMSO	5 μγ/ml MMS	15 μg/ml MMS	3 μg/ml CP	5 μg/ml CP
Without S9	45.9	46.1	49.5	44.8	199.5	390.0	N/A	N/A
With S9	40.6	35.1	47.1	73.1	N/A	N/A	276.2	490.8

Mutant frequency ($x10^{-6}$).

was observed for all strains with the appropriate positive control compared with negative controls. Negative control reversion rates for each strain were within expected or lower ranges of historical laboratory data. Each of the test strains was confirmed for genotypic markers and acceptable spontaneous reversion rates to ensure they maintained the characteristics which make them sensitive to mutagenic activity (data not shown). These observations indicate a valid assay. Furthermore, no substantial toxicity was noted due to ntSPONGE™ extract exposure which may have interfered with the assay. None of the tester strains showed an increase in reversion rates when treated with ntSPONGE™ extract.

Mouse lymphoma assay. The mouse lymphoma assay was used to determine if ntSPONGE™ was capable of inducing either point mutations or clastogenic events in a cultured mammalian cell line. The use of the metabolic activation system (S9) was included as some mutagenic compounds may exist in a pro-mutagenic state. The mutant frequencies and cloning efficiencies of the cells treated with the test article were within the limits defined for a negative response. In addition, the saline and DMSO controls for the assay performed as required thereby qualifying both the assay and culture systems. As shown in **Table 4**, extracts from ntSPONGE did not show any increase in mutant frequency when compared with the carrier controls.

Systemic toxicity. Acute systemic injection test was used to evaluate the systemic toxicity of ntSPONGE. **Table 5** shows the summary of results for systemic toxicity of the extracts in mice. None of the ntSPONGE-extract treated animals showed adverse clinical signs at any of the observation periods and none of the animals lost in excess of 10% of their body weight over the course of the study.

Subacute intraperitoneal injection toxicity. The subacute intraperitoneal injection toxicity assay was used to investigate the effects of an extract from ntSPONGE in mice. Repeated dosing insures longer term exposure of the material leachables than the acute systemic toxicity test described above. **Table 6A and B** summarizes the data obtained from these studies. All treated and control animals survived the 14-d dosing regimen. All of the male and female animals in both the control and treated groups appeared normal throughout the duration of the study. The abnormal lesions (white spots) observed on the peritoneal surfaces and abdominal organs of all the animals in most likely peritonitis. It is commonly observed in laboratory mice where cottonseed oil is used as the vehicle for intraperitoneal administration. All test and control animals otherwise, appeared macroscopically normal. All animals gained weight throughout the study (**Table 6B**). There was no difference between the treated and control mice at any of the recorded times in the study.

Table 5. Acute Systemic Toxicity of ntSPONGE™

Extract	Fatalities		Clinical Signs of Toxicity		> 10% Body Weight Loss	
	ntSPONGE	Control	ntSPONGE™	Control	ntSPONGE™	Control
NS	0/5	0/5	0/5	0/5	0/5	0/5
CSO	0/5	0/5	0/5	0/5	0/5	0/5

Fatalities, toxicity signs, and weight loss greater than 2 g in mice systemically exposed to ntSPONGE™ and control extracts.

Table 6A. Clinical Observations of Subacute Intraperitoneal Toxicity

Group	Fatalities		Clinical Signs of Toxicity		Abnormal Lesions Noted at Necropsy	
	ntSPONGE	Control	ntSPONGE™	Control	NntSPONGE™	Control
Male	0/5	0/5	0/5	0/5	*5/5	*5/5
Female	0/5	0/5	0/5	0/5	*5/5	*5/5

*White spots were noted throughout the abdomen.

Table 6B. Mean + Standard Deviation Body Weight and Body Weight Change (g) of Subacute Intraperitoneal Toxicity

Article	Male			Female		
	Day 0	Day 14	Change	Day 0	Day14	Change
Control	24.4 ± 1.68	32.7 ± 2.15	8.4 ± 1.45	21.3 ± 0.90	24.2 ± 1.25	2.9 ± 1.15
Test	24.5 ± 1.26	32. ± 0.54	8.2 ± 0.99	21.3 ± 1.17	23.5 ± 1.08	2.2 ± 0.39

Table 7A. Clinical Observations of Subchronic Intravenous Toxicity

Group	Fatalities		Clinical Signs of Toxicity		Abnormal Lesions Noted at Necropsy	
	ntSPONGE	Control	ntSPONGE™	Control	ntSPONGE™	Control
Male	0/5	0/5	0/5	0/5	0/5	0/5
Female	0/5	0/5	0/5	0/5	0/5	0/5

Table 7B. Mean + Standard Deviation Body Weight and Body Weight Change (g) of Subchronic Intravenous Toxicity

Article	Male			Female		
	Day 0	Day 14	Change	Day 0	Day14	Change
Control	25.8 ± 2.14	31.8 ± 0.97	6.0 ± 1.55	21.4 ± 1.82	23.2 ± 1.75	1.8 ± 0.79
Test	26.1 ± 2.01	32.8 ± 3.59	6.7 ± 1.98	21.2 ± 1.71	23.0 ± 2.00	1.7 ± 0.87

Subchronic intravenous toxicity. These studies were performed to investigate the subchronic toxicity of extracts of ntSPONGE in mice. As in the intraperitoneal study described above, repeated doses were administered to insure longer exposure times to the leachable materials from ntSPONGE. All animals were alive at the end of the study. As shown in **Table 7A**, there were no clinical signs of toxicity and no abnormal lesions were observed at necropsy. All the males and females gained weight throughout the study (**Table 7B**).

Histological evaluation. Samples of ntSPONGE™ were fixed in formalin and embedded in paraffin, sectioned and stained. As shown in **Figure 1A**, there is no residual cellular debris as detected by the H&E staining. The ribbons of collagen are clearly visualized. As shown in **Figure 1B**, the starting material demonstrated very little glycosaminoglycan (GAGs) staining with Alcian Blue. In contrast, ntSPONGE™ was clearly stained blue indicating the presence of cross-linked HA. HA was distributed evenly as indicated by the blue staining that was observed throughout the material.

Morphology. The cross-sectional images demonstrate that the porous structure of the collagen scaffold was largely preserved after cross-linking in the presence of EDC (**Fig. 2A–C**). After cross-linking, more sheet-like structures were observed and the pore sizes were approximately 100 μm.

Ultimate tensile strength. The results of the tensile testing of non-cross-linked and cross-linked collagen matrices are presented in **Figure 3**. The results presented are an average from 5 different samples tested. No significant difference in ultimate tensile strength was observed between the cross-linked and non-cross-linked material.

Cross-linking determination. To determine the effects of the cross-linking and the relative cross-linking density on ntSPONGE™, DSC and pronase resistance analyses were performed. As shown in **Table 8A**, ntSPONGE™ demonstrated a consistently higher denaturation point when compared with the non-cross-linked material. The enzymatic biodegradation results of the cross-linked scaffold in presented in **Table 8B**. The non-cross-linked scaffold was completely digested when incubated in pronase solution at 50 °C for 24 h. However, 80% of the ntSPONGE™ material remained resistant to pronase degradation indicating that the EDC treatment conferred resistance to pronase degradation.

Cell attachment and proliferation. The ability of cells to attach and proliferate on the ntSPONGE™ material was investigated over a 10-d period. As shown in **Figure 4**, the cell numbers increased over time throughout the 10-d incubation period. **Figure 4A** demonstrates that cells are able to proliferate on the ntSPONGE™ in a similar manner as when grown on tissue culture plastic. The cells were observed directly attached to the ntSPONGE™ (**Fig. 4B**). In addition, the cells were able to proliferate in and around the ntSPONGE™ as shown with the number of viable cells in the original wells.

Rabbit intramuscular implantation. All animals survived to the scheduled study endpoint. No abnormal clinical signs were noted for any of the animals throughout the course of the study. All samples were scored normal from macroscopic observataions. Histological examination of the explants showed that the non-cross-linked material was > 90% resorbed at the end of two weeks (**Fig. 5A**). In contrast, the ntSPONGE™ material (cross-linked) was partially intact at the end of the study as noticed by the interconnected spicules of homogeneous acellular material (**Fig. 5B**). The non-cross-linked material was characterized by a mild tissue capsule response of fibroblasts and soft tissue with mild neovascularization (**Table 9A**, see **Table 9E** for scoring criteria). The samples also demonstrated moderate to marked tissue ingrowth into the device seen as fibrovascular connective tissue. All of the samples had mild to moderate numbers of PMNs, and marked number of lymphocytes and macrophages. The ntSPONGE™ samples were characterized by a mild to moderately thick capsule of fibroblasts and collagen with signs of neovascularization (**Table 9B**). All samples had mild tissue ingrowth into the device seen as fibrovascular connective tissue. In addition, each site had minimal to moderate numbers of lymphocytes and macrophages infiltrating the capsule. Minimal numbers of PMNs and giant cells were also observed.

At 16 weeks, all but two of the non-cross-linked test sites did not contain any visible sample material and mainly contained normal tissue. The two samples that were observed had minimal thin homogeneous ribbons (**Fig. 5C**). The inflammation that was observed was characterized by lymphocytes and macrophages with an occasional giant cell (**Table 9C**). The ntSPONGE™ samples were observed in 11 of the 15 sites at 16 weeks. All of these sites were similar histologically (**Table 9D**). Each of the samples were surrounded by a narrow band (< 100 μm) of fibrous tissue capsule composed of fibroblasts and soft tissue with a minimal amount of neovascularization (**Fig. 5D**). All of these sites also had minimal to marked tissue ingrowth and cellular infiltration containing lymphocytes, macrophages, PMNs, and giant cells. The remaining sites did not contain any visible test article.

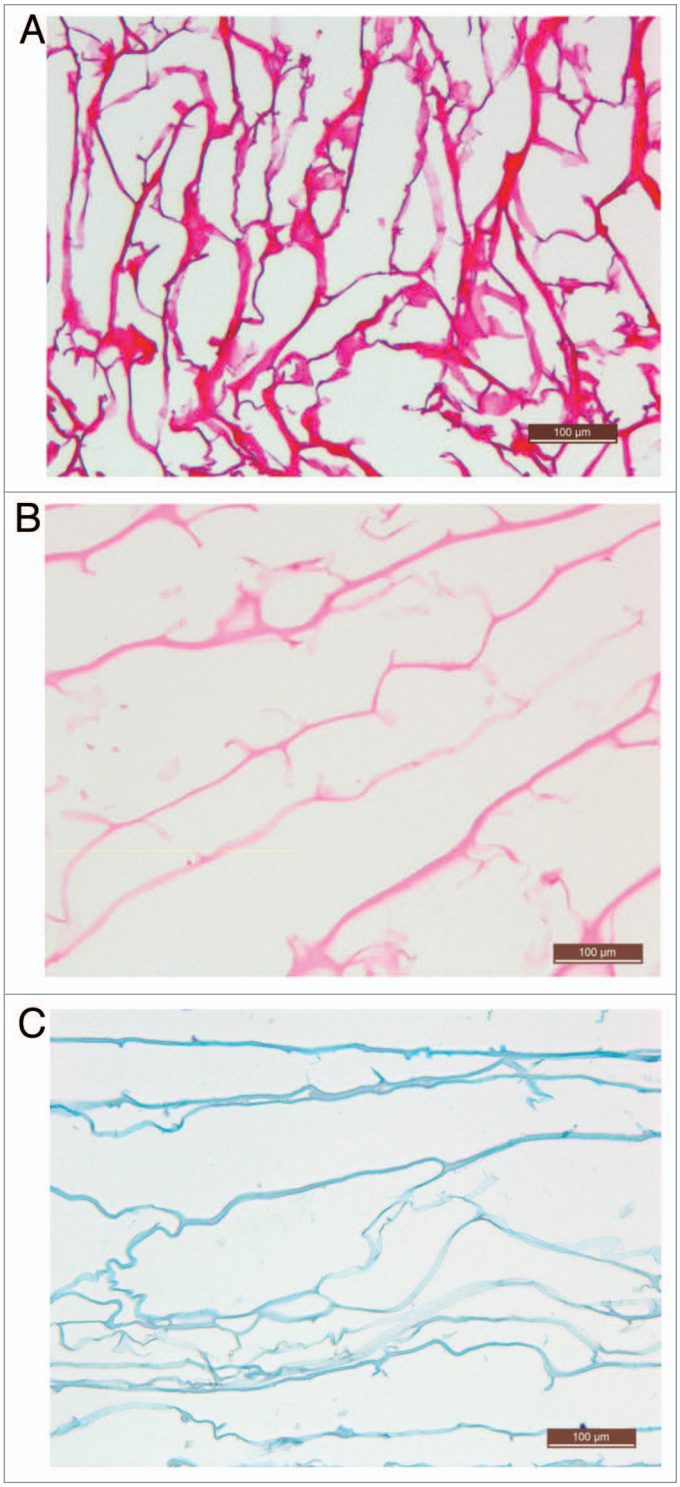

Figure 1. Cross-sectional view of ntSPONGE™ embedded with paraffin. Five micron sections were cut and then stained. (**A**) ntSPONGE™ stained with H&E; (**B**) Starting material stained with Alcian Blue; (**C**) ntSPONGE™ stained with Alcian Blue. Three different batches were examined and a representative slide is presented at magnification of 10x.

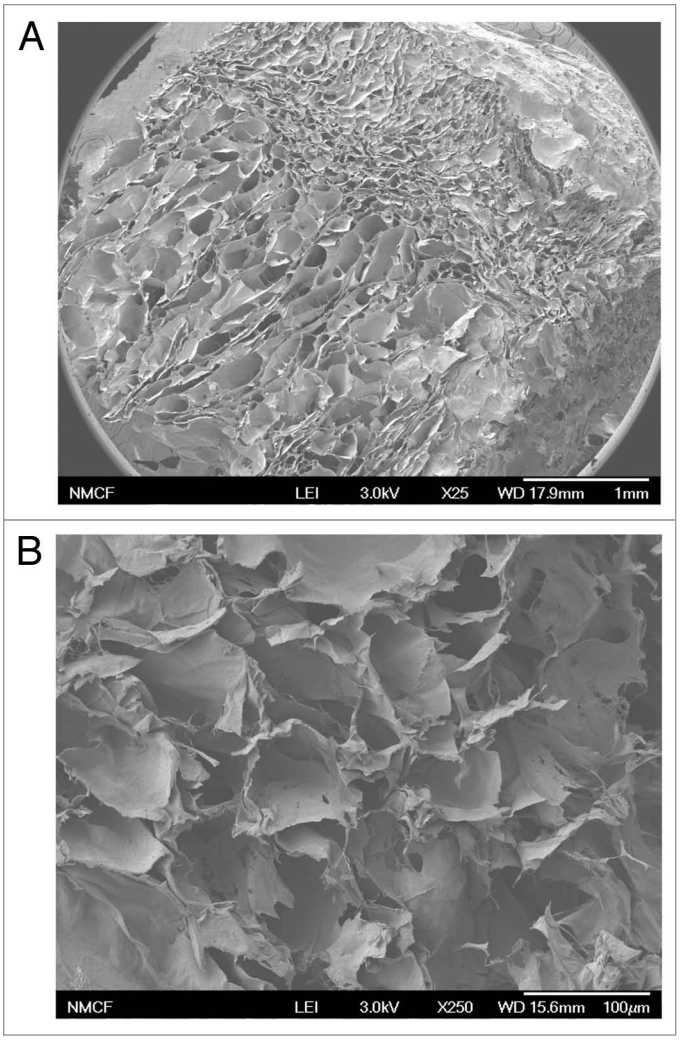

Figure 2. SEM of ntSPONGE™ ™ components. Three samples of each were analyzed and representative micrographs are shown. (**A**) Magnification of 25x; (**B**) magnification of 250x

Discussion

The range of biomaterials commercially available for the treatment of venous leg ulcers and diabetic foot ulcers has increased over the past ten years. Tissue engineering is now showing promise as a possible method for wound healing and seeking a suitable scaffold has become more and more important. While water soluble carbodiimides, such as EDC, have been used in protein conjugation chemistry for over three decades, its use in cross-linking collagen-based materials is more recent.[39–44] This study evaluated an EDC cross-linked collagen sponge, ntSPONGE™, in several in vitro model systems. Hyaluronic acid was covalently attached to the collagen fibers using EDC. The EDC immobilizes the HA and stabilizes the collagen by formation of amide cross-links.[30]

The disadvantages of using reconstituted collagen or collagen-HA composites as a scaffold for tissue regeneration are their rapid degradation and clearance. Hence, to stabilize the structure of these natural polymers various chemical and/or physical cross-links are frequently introduced. Non-cross-linked material was shown to be much more sensitive to protease degradation compared with EDC cross-linked material. In addition, the denaturation temperature of the EDC cross-linked material (ntSPONGE™) was also higher than that observed with non-cross-linked materials. These results are consistent with those of previously described investigating similar materials.[42,43]

The data presented herein demonstrates that the ntSPONGE™ is capable of providing a scaffold for cells to attach and proliferate in the absence of cytotoxicity in a similar manner as described.[42,43] The porous nature of the ntSPONGE™ was very similar to that observed in previous studies.[42–44] The porous structure allows for cells to attach and proliferate which is required for wound healing. Unlike glutaraldehyde cross-linked collagen which is usually associated with cytotoxicity both in vitro and in vivo, the use of EDC as the cross-linking agent yields biomaterials with good biocompatibility, higher cellular differentiation potential, and increased stability.[45–47]

Another characteristic of a clinically relevant wound healing device is that it should be biocompatible and non-cytotoxic. It is evident from the data presented herein that the process to generate the EDC cross-linked collagen sponge that contains HA did not result in a material that exhibited cytotoxic or genotoxic effects. No cytotoxic effects were observed when a mouse fibroblast cell line was exposed to the material. No genotoxic/mutagenic effects were observed in the Ames assays or the mouse lymphoma assays under the conditions used herein. The ntSPONGE™ was also evaluated for toxic effects in several animal models. Extracts derived from the material did not elicit any observable adverse events in an acute toxicity model in mice. In addition, no adverse events were observed in a subacute intravenous and intraperitoneal toxicity assays measured in mice. **Table 10** provides an overview of the biocompatibility test results. From these results, the process used to generate the EDC cross-linked collagen sponge that contains HA results in a biocompatible product. The results clearly demonstrate that the material does not contain any residual compounds that would result in a toxic effect in the animals.

The ability of the material to be resorbed was analyzed in an intramuscular implantation study conducted in New Zealand White rabbits. The cross-linked material was directly compared with a non-cross-linked, sterile collagen dressing material. There was a clear difference in the resorbtion times observed between the two materials. The interconnected fibers of the ntSPONGE™ were clearly visible at the two week time point and in some samples at the 16 week time point. There was clear evidence of neovascularization in the ntSPONGE™ sample as compared with the control sample. Additionally, an increased number of infiltrating fibroblasts were observed on the ntSPONGE™ samples compared with the control sample. Much less fatty scar tissue was observed in the ntSPONGE™ samples compared with the control sample. Taken together, we reasonably conclude that the cross-linked material represents a more stable material compared with the non-cross-linked material when used in vivo.

The data presented herein also demonstrates that the process to generate the EDC cross-linked collagen sponge that contains

HA resulted in the homogenous deposition of the HA throughout the collagen fibers. The process did not result in any adverse effects on the collagen structure or pore size. These characteristics are important for cell binding, migration and proliferation. In addition, the cross-linking process did not adversely affect the biomechanical strength of the collagen scaffold.

Wound healing is dependent on the activity of the surrounding fibroblast and keratinocyte cells and their precursors. Migration and proliferation of these cells is influenced by the interaction of the surface of the wound with cells. The attachment and proliferation of these cells is dependent on the surface porosity and extracellular matrix content. The surface of ntSPONGE™ was shown to be porous and the data presented demonstrates that ntSPONGE™ supports the attachment and proliferation of fibroblasts. It is important for the ntSPONGE™ material to support the growth of these cells because these cells and their precursors are responsible for wound healing.

Taken together, the results presented herein indicate that EDC cross-linking and the covalent attachment of HA results in a collagen scaffold (ntSPONGE™) that can resist the environment of a chronic wound, can support cell growth and attachment and is biocompatible. These data support the potential use of ntSPONGE™ as a promising wound care device for use in the treatment of venous leg ulcers and diabetic foot ulcers.

Materials and Methods

Wound dressing material. The base scaffold used for this preparation was a collagen sponge derived from equine tendons by standard acetic acid extraction and freeze drying (Euroresearch, srl). The collagen was covalently cross-linked by EDC followed by a hyaluronic acid (HA) cross-linking step with a ratio of 0.5 mg of hyaluronic acid per 1mg of collagen. Terminal sterilization was achieved with electron beam radiation to provide a sterility assurance level of 10^{-6} (SAL 10^{-6}). All biocompatibility tests were performed by WuXi Apptec. All extractions of the test articles were performed in the appropriate solutions at 37 °C with agitation unless otherwise stipulated. Extracts were stored at 6 °C and were used within 24 h of preparation. All animal studies were approved by WuXi AppTec IACUC prior to initiation of all procedures.

Cytotoxicity. Cytotoxic effects of ntSPONGE™ were evaluated with the test protocol ISO MEM Elution Using L-929 Mouse Fibroblast Cells. The ntSPONGE™ material was extracted with Eagle's Minimal Essential Medium (E-MEM) supplemented with 5% Fetal Bovine Serum (FBS) at 37 ± 1 °C for 24–25 h. The maintenance culture media was removed from the monolayer in the test culture wells and replaced with 1 mL of test media/extract, control media/extract or positive control media spiked with $CdCl_2$. Positive, intermediate, and negative controls were run in parallel with the test articles and all treatments were plated in triplicates. Cell cultures were incubated 72 ± 4 h at 37 ± 1°C in a humidified atmosphere of 5 ± 1% CO_2 in air. Cultures were evaluated for cytotoxic effects by microscopic observation after 24, 48, and 72 ± 4 h incubation periods. Criteria for evaluating cytotoxicity include morphological changes in cells, such as granulation, crenation, or rounding, and loss of viable cells from the monolayer by lysis or detachment (**Table 1**).[48]

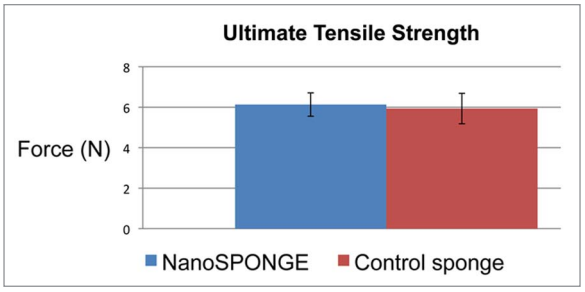

Figure 3. Ultimate tensile strength of ntSPONGE™. The results from 5 different samples were averaged and presented.

Table 8A. DSC Evaluations of Relative Cross-Linking Density

Sample	Average Denaturation Temperature
1	67.12°C
2	69.56°C
3	70.54°C
Control	49.14°C

Each sample was evaluated at least 3 times. The average denaturation temperature of the different analyses is given. The control is the non-cross-linked starting material for the ntSPONGE™ material. Samples 1–3 represent different lots of ntSPONGE™.

Table 8B. Pronase Resistance Analyses of Relative Cross-Linking Density

Sample	Pre-Exposure (mg)	Post-Exposure (mg)	% Mass Remaining
1	33.7	26.1	76.8
2	33.2	27.1	81.7
3	27.7	22.6	80.3
Control	23.8	0	0.0

The data are given as an average of the six replicates. The control sample was the non-cross-linked starting material. Samples 1–3 represent different lots of ntSPONGE™.

Genotoxicity/mutagenicity. Mutagenicity of extracts of the test samples were evaluated using the assay originally developed by Ames et al.[49] and five different strains of *S. typhimurium* (TA97A, TA98, TA100, TA102, and TA1535). This is an incorporation assay in the presence and absence of an exogenous mammalian activation system (S9). Frozen working stocks were used to create working cultures of each bacterial strain. Cultures were grown overnight at 37 ± 2 °C until a density of 0.6–1.6 at 650 nm was reached. ntSPONGE™ extract or vehicle control plus bacteria culture plus either PBS or metabolic activation solution (S9) was added to a molten top agar of 0.6% Difco agar in 0.5% NaCl supplemented with an L-histidine/0.5 mM biotin solution. The solution was vortexed and allowed to harden and incubated for 48 -72 h at 37 ± 2 °C. All plates were scored using an automatic image analysis (Domino Image Analyzer) system

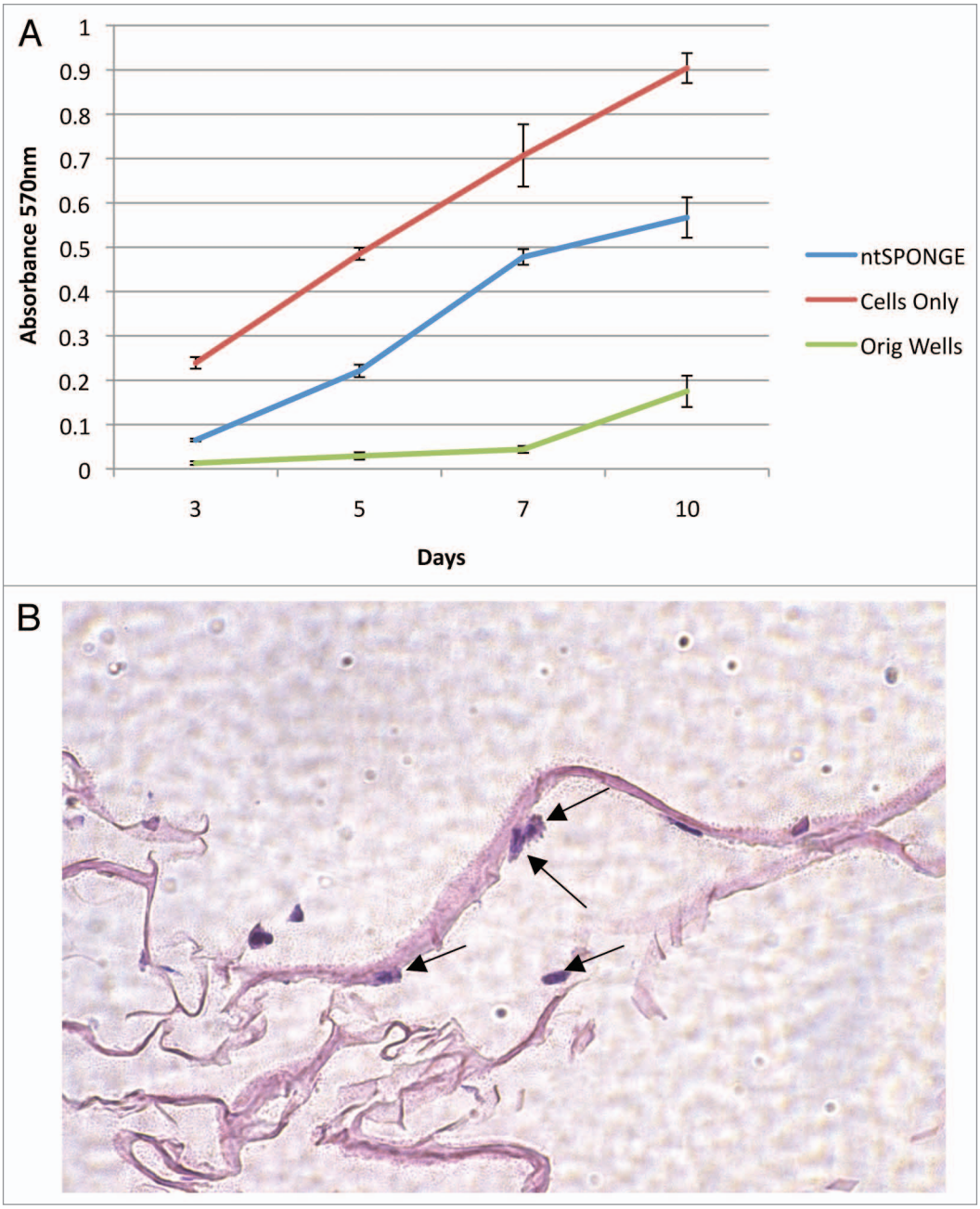

Figure 4. Cell attachment and proliferation on ntSPONGE™. Cell numbers were determined at day 3, 5, 7 and 10 d post seeding using MTT reagent. Cells were allowed to incubate with and without ntSPONGE™ material in the wells. At each timepoint, the ntSPONGE™ material was removed and counted separately (ntSPONGE™). The wells that contained the ntSPONGE™ material was also counted separately (orig. wells). (**A**) Mouse L929 cell proliferation on ntSPONGE™. (**B**) Mouse L929 cells attached directly to the ntSPONGE™. The ntSPONGE™ was removed from the wells at each time point, fixed in paraformaldehyde and stained with H&E. Representative samples are shown (magnification = 200x). Arrows refer to cells attached directly to ntSPONGE™.

for colony counting. Negatives controls were plated with normal saline (NS) or DMSO extraction blanks, with and without S9.

Mouse lymphoma assay. The assay procedures used were based on those developed by Clive et al.[50,51] The test materials were extracted in normal saline or DMSO for 72 h at 37 °C. The saline test article and saline negative control were dosed in 1.0 mL volumes while the DMSO test article and control were dosed at 0.1 mL volumes. A total of 6×10^6 cells in a final volume of 10 mL (cells plus test article) were incubated at 37 °C on a shaking incubator (80 rpm) for 4 h. The cells were then washed once and resuspended in 20 mL media and incubated for 48 h. Prior to cloning, cells were adjusted to a final density of 2×10^5 cells/mL in 20 mL of media. Mutagenicity was determined by suspending 5 mL from each dose tube (1×10^6 total cells) in the cloning media. Three plates were prepared from each tube. After 11 d of incubation at 37 °C, the colonies were counted using

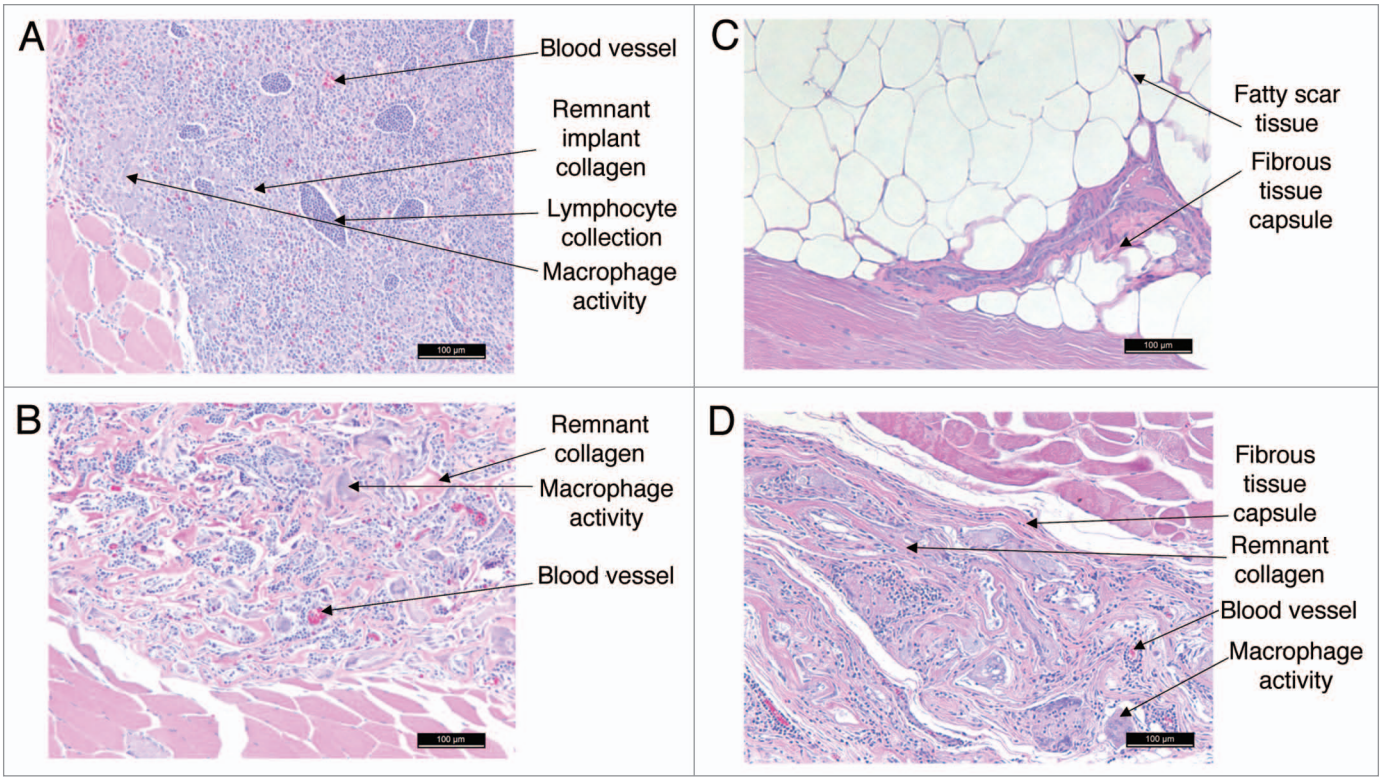

Figure 5. Intramuscular Implantation of ntSPONGE™. Samples were implanted into the paravertebral muscles of New Zealand White rabbits. Animals were sacrificed and explants were removed. The muscle tissue was fixed in 10% buffered formalin and embedded with paraffin. Slides were stained with H&E and evaluated histologically. Three different samples were evaluated and a representative slide is presented (10x magnification). (**A**) Two week sample, non-cross-linked starting material; (**B**) Two week sample, ntSPONGE™; (**C**) Sixteen week sample, non-cross-linked starting material; (**D**) Sixteen week sample, ntSPONGE™.

a Domino Image Analyzer including software for colony size discrimination.

Systemic toxicity. Systemic toxicity of ntSPONGE™ was evaluated with the test protocol ISO Acute Systemic Injection Test. Twenty mice were injected systemically with two extracts of ntSPONGE™ (normal saline [NS] or cottonseed oil [CSO]) or the appropriate vehicle. Animals were observed for fatality/signs of toxicity immediately after injection and at 4, 24, 48, and 72 h post-injection. Animals were also monitored for weight loss. Subchronic intravenous toxicity was evaluated using 20 mice. Animals were injected intravenously daily for 14 d at a dose of 10 ml/kg. Observations for mortality and clinical signs of pharmacologic and/or toxicologic effects were made immediately post-injection and once a day for 14 d. Blood samples were drawn on day 14 via cardiac puncture. Gross necropsy was also performed. Subacute intraperitoneal toxicity was evaluated using 20 mice. Animals were injected intraperitoneally daily for 14 d at a dose of 1ml/kg in cottonseed oil. Animals were observed immediately post-injection and daily for 14 d for mortality and clinical signs of toxicologic and pharmacologic effects. Blood samples were obtained on day 14 by cardiac puncture. Gross necropsy was performed on each animal.

Intramuscular implant test. The local effects of ntSPONGE™ were evaluated in New Zealand White rabbits. A total of 30 ntSPONGE™ samples and 30 non-cross-linked samples were evaluated. A total of 5 of each were implanted into each animal Three animals were used for each time point (2 weeks and 16 weeks). Animals were anesthetized with a combination of 20–40 mg/kg of ketamine hydrochloride and 0.5–1.0 mg/kg of acepromazine. Supplemental isoflurane gas anesthesia was also used. The fur on the animals was shaved on either side of the spine. The surgical site was scrubbed with Betadine solution and cleaned with 70% isopropanol. A single incision was made in the skin along the mid-line of the animals back. The upper layers of fascia were also incised to expose the paravertebral muscles. A small incision was made to accommodate the size of the implant. Five samples of ntSPONGE™ were implanted in the right paravertebral muscles and five samples of the control were implanted in the left paravertebral muscles. The surgical sites were closed with absorbable suture and the skin was closed with skin staples. The rabbits were sacrificed by lethal injection of sodium pentobarbital (Euthsol) at the end of the two week and 16 week periods. Tissue samples from each surgical implant site were explanted and fixed in 10% neutral buffered formalin. Samples were embedded in paraffin, sectioned and stained with hematoxylin and eosin. Samples were evaluated for inflammation via cell counts for polymorphonuclear cells (PMNs), lymphocytes, plasma cells, eosinophils, macrophages, multinucleated giant cells and necrosis (**Table 9E** for scoring criteria). Samples were also evaluated for tissue response by observing neovascularization, fibrosis/fibrous

Table 9A. Two week non-cross-linked samples of inflammation and tissue response to implant sites

Animal number			**1**					**2**					**3**		
Implant site	1	2	3	4	5	1	2	3	4	5	1	2	3	4	5
Inflammation (I)															
0PMNs	3	2	3	3	2	3	3	2	2	2	3	3	4	4	2
Lymphocytes	4	4	4	4	4	4	4	4	4	4	4	4	4	4	4
Plasma cells	0	0	0	0	0	0	0	0	0	0	0	0	0	0	0
Eosinophils	0	0	0	0	0	0	0	0	0	0	0	0	0	0	0
Macrophages	4	4	4	4	4	4	4	4	4	4	4	4	4	4	4
Giant cells	2	0	0	1	1	2	0	0	1	1	2	2	2	1	1
Necrosis	0	0	0	0	0	0	0	0	0	0	0	0	0	0	0
Total (I)	**13**	**10**	**11**	**12**	**11**	**13**	**11**	**10**	**11**	**11**	**13**	**13**	**14**	**13**	**11**
Tissue response (TR)															
Vascularizatin	2	2	2	2	2	2	2	2	2	2	2	2	2	2	2
Fibrous capsule	1	1	1	1	1	1	1	1	1	1	1	2	1	2	1
Granuloma formation	0	0	0	0	0	0	0	0	0	0	0	0	0	0	0
Tissue in-growth	4	3	4	3	4	0	4	3	3	3	4	3	3	4	3
Total (TR)	**7**	**6**	**7**	**6**	**7**	**3**	**7**	**6**	**6**	**6**	**7**	**7**	**6**	**8**	**6**
Total (I+TR)	**20**	**16**	**18**	**18**	**18**	**16**	**18**	**16**	**17**	**17**	**20**	**20**	**20**	**21**	**17**
Mean fibrous capsule thickness (μm)	0	0	0	0	0	0	0	0	0	0	0	0	0	0	0

Table 9B. Two week ntSPONGE™ samples of inflammation and tissue response to implant sites

Animal number			**1**					**2**					**3**		
Implant site	1	2	3	4	5	1	2	3	4	5	1	2	3	4	5
Inflammation (I)															
PMNs	1	1	1	1	1	2	1	1	1	2	1	1	0	1	1
Lymphocytes	2	2	2	2	2	3	3	3	3	3	1	2	1	2	2
Plasma cells	0	0	0	0	0	0	0	0	0	0	0	0	0	0	0
Eosinophils	0	0	0	0	0	0	0	0	0	0	0	0	0	0	0
Macrophages	1	1	1	2	1	2	1	1	1	1	1	1	1	2	1
Giant cells	1	1	1	1	0	1	1	1	1	1	1	1	1	1	1
Necrosis	0	0	0	0	0	0	0	0	0	0	0	0	0	0	0
Total (I)	**5**	**5**	**5**	**6**	**4**	**8**	**6**	**6**	**6**	**7**	**4**	**5**	**3**	**6**	**5**
Tissue response (TR)															
Vascularizatin	2	1	1	1	1	1	1	1	1	1	1	1	1	2	1
Fibrous capsule	1	1	1	1	1	2	1	1	1	1	2	1	1	3	1
Granuloma formation	0	0	0	0	0	0	0	0	0	0	0	0	0	0	0
Tissue in-growth	2	2	2	2	2	2	2	2	2	2	2	2	2	2	2
Total (TR)	**5**	**4**	**4**	**4**	**4**	**5**	**4**	**4**	**4**	**4**	**5**	**4**	**4**	**7**	**4**
Total (I+TR)	**10**	**9**	**9**	**10**	**8**	**13**	**10**	**10**	**10**	**11**	**9**	**9**	**7**	**13**	**9**
Mean fibrous capsule thickness (μm)	**0**	0	0	0	0	0	0	0	0	0	0	0	0	0	0

Table 9C. Sixteen week non-cross-linked samples of inflammation and tissue response to limplant sites

Animal number			**1**					**2**					**3**		
Implant site	**1**	**2**	**3**	**4**	**5**	**1**	**2**	**3**	**4**	**5**	**1**	**2**	**3**	**4**	**5**
Inflammation (I)															
PMNs	0	0	1	0	1	0	0	0	0	0	0	0	0	0	0
Lymphocytes	3	0	3	0	3	3	0	4	0	0	3	4	0	3	4
Plasma cells	0	0	0	0	0	0	0	0	0	0	0	0	0	0	0
Eosinophils	0	0	0	0	0	0	0	0	0	0	0	0	0	0	0
Macrophages	2	0	1	3	3	3	0	3	0	0	0	1	0	0	3
Giant cells	0	0	1	0	1	0	0	0	0	0	0	0	0	0	1
Necrosis	0	0	0	0	0	0	0	0	0	0	0	0	0	0	0
Total (I)	**5**	**0**	**6**	**3**	**8**	**6**	**0**	**7**	**0**	**0**	**3**	**5**	**0**	**3**	**8**
Tissue response (TR)															
Vascularization	0	0	0	0	0	0	0	0	0	0	0	0	0	0	0
Fibrous capsule	0	0	0	0	0	0	0	0	0	0	0	0	0	0	0
Granuloma formation	0	0	0	0	0	0	0	0	0	0	0	0	0	0	0
Tissue in-growth	0	0	0	0	0	0	0	0	0	0	0	4	0	0	4
Total (TR)	**0**	**0**	**0**	**0**	**0**	**0**	**0**	**0**	**0**	**0**	**0**	**4**	**0**	**0**	**4**
Total (I+TR)	**5**	**0**	**6**	**3**	**8**	**6**	**0**	**7**	**0**	**0**	**3**	**9**	**0**	**3**	**12**
Mean fibrous capsule thickness (μm)	0	0	0	0	0	0	0	0	0	0	0	0	0	0	0

Table 9D. Sixteen week ntSPONGE™ samples of inflammation and tissue response to implant sites

Animal number			**1**					**2**					**3**		
Implant site	**1**	**2**	**3**	**4**	**5**	**1**	**2**	**3**	**4**	**5**	**1**	**2**	**3**	**4**	**5**
Inflammation (I)															
PMNs	0	0	0	0	1	1	1	1	1	1	0	0	0	0	0
Lymphocytes	1	3	0	2	3	3	4	4	4	4	1	2	0	0	3
Plasma cells	0	0	0	0	0	0	0	0	0	0	0	0	0	0	0
Eosinophils	0	0	0	0	0	0	0	0	0	0	0	0	0	0	0
Macrophages	1	3	2	0	3	1	1	1	1	1	0	1	1	0	2
Giant cells	0	0	0	0	0	1	1	1	2	2	0	1	0	0	0
Necrosis	0	0	0	0	0	0	0	0	0	0	0	0	0	0	0
Total (I)	**2**	**6**	**2**	**2**	**7**	**6**	**7**	**7**	**8**	**8**	**1**	**4**	**1**	**0**	**5**
Tissue response (TR)															
Vascularizatin	0	1	0	0	1	1	1	1	1	1	1	1	0	0	0
Fibrous capsule	0	1	0	0	1	1	1	1	1	1	1	1	0	0	1
Granuloma formation	0	0	0	0	0	0	0	0	0	0	0	0	0	0	0
Tissue in-growth	0	3	0	0	0	4	1	3	2	3	0	0	0	0	0
Total (TR)	**0**	**5**	**0**	**0**	**2**	**6**	**3**	**5**	**4**	**5**	**2**	**2**	**0**	**0**	**1**
Total (I+TR)	**2**	**11**	**2**	**2**	**9**	**12**	**10**	**12**	**12**	**13**	**3**	**6**	**1**	**0**	**6**
Mean fibrous capsule thickness (μm)	0	20	0	0	12	27	12	8	20	30	80	33	0	0	20

Table 9E. Severity Scores of Inflammation and Tissue Response to Implant Sites

Inflammation	Score				
	0	**1 = Minimal**	**2 = Mild**	**3 = Moderate**	**4 = Marked**
PMNs Lymphocytes Plasma cells Eosinophils Macrophages	0	Rare, 1–5/HPF*	6–10/HPF	Heavy Infiltrate	PAcked
Giant cells	0	Rare 1–2/HPF	3–5/HPF	Heavy Infiltrate	Sheets
Necrosis	0	Minimal	Mild	Moderate	Severe
Tissue response	**Score**				
	0	**1 = Minimal**	**2 = Mild**	**3 = Moderate**	**4 = Marked**
Vascularizatin	Absent	Minimal capillary proliferation or small blood vessels (1–3 capillary buds)	Groups of 4–7 capillaries with supporting fibroblastic structures	Broad band of capillaries with supporting structures	Extensive band of capillaries with supporting structures
Fibrous capsule	Fibrous capsule is not formed or is too thin to measure	Narrow band (≤ 100mm mean capsule thickness)	Moderately thick band (> 100mm, up to 200mm mean capsule thickness)	Thick band (> 200 mm up to 300 mm mean capsule thickness)	Extensive band (> 300 mm mean capsulte thickness)
Granuloma formation	Absent	Minimal/slight (> 0 up to 25% fo the implant field)	Mild (> 25 up to 50% of the implant field)	Modereate (> 50–75% of the implant field)	Marked/Severe (> 75% of the implant field)
Tissue in-growth	Absent	Minimal/slight (> 0 up to 25% fo the implant field)	Mild (> 25 up to 50% of the implant field)	Modereate (> 50–75% of the implant field)	Marked/Severe (> 75% of the implant field)

*High powered field (400x total magnification)

capsule, granuloma formation and tissue in-growth into the materials.

Cell attachment and proliferation. Samples of the ntSPONGE™ were hydrated with DMEM media containing 10%FCS and cut out as 1 cm diameter disks. Each disk was placed in a well of a 48-well plate. L929 cells (ATCC) were seeded onto the wells containing ntSPONGE™ and control wells without ntSPONGE™ (1×10^4 cells/well). The media was renewed every third day. MTT assays were performed using quadruplicated wells on each time point by following the protocol provided by the manufacturer (Life Technologies). The ntSPONGE™ samples were removed from the wells and analyzed separately. The wells where the ntSPONGE™ was removed was counted as analyzed as well (orig. wells in the figure). To demonstrate that the cells were attached directly to the ntSPONGE™ material, the ntSPONGE™ was removed from the wells at each time point, fixed in paraformaldehye and stained with hematoxylin and eosin. Representative samples are shown in figures.

Scanning electron microscopic analysis. Formalin fixed samples were dried, mounted and sputter coated with platinum. Micrographs of each sample were then obtained with a scanning electron microscope (SEM) (JEOL 6700). Dry samples were prepared by direct adhesion to standard "1" Aluminum SEM mounts and sputter coated with gold in a precision etching and coating system (PECS) Gatan Model 681. The analyses were performed at an accelerating voltage of 5 kV.

Table 10. Biocompatibility test results

Test	Result
Cytotoxicity	Non-cytotoxic
Intracutaneous Reactivity	Non-irritant
Acute Systemic Toxicity	Non-toxic
Sub-acute Toxicity	Non-toxic
Sub-chronic Toxicity	Non-toxic
Hemolysis	Non-hemolytic
Material Mediated Pyrogenicity	Non-pyrogenic
Genotoxicity: Reverse Mutation	Non-mutagenic
Genotoxicity: Mouse Lymphoma	Non-mutagenic
Intramuscular Implant	Non-irritant

Histological evaluations. Representative samples of the non-cross-linked and cross-linked collagen matrices were evaluated microscopically using standard histological methods. All samples were fixed in 10% neutral buffered formalin, embedded in paraffin, cut into 5 μm sections, mounted on slides and stained with standard histological techniques. Non-implanted tissue sections were stained with hematoxylin and eosin (H&E), Verhoeff-Van Gieson, and alcian blue techniques (Laudier Histology).

Cross-linking determination. Two different analyses were used to determine the effects of cross-linking on the collagen material. All differential scanning calorimetry (DSC) was

performed using a Mettler Toledo DSC 823, EL-099. Samples to be analyzed were soaked in normal saline solution. A thin piece of the material was cut (approximately 3 × 3 × 1 mm) and then blotted to remove excess moisture. The sample was then analyzed over 40–120 °C at 30 °C/min heating rate. Each sample was analyzed at least three times. Pronase digestion was performed to determine the ability of the ntSPONGE™ dressing to resist break down by proteolytic enzymes. ntSPONGE™ was exposed to pronase (Sigma) (25 mg/ml) at 50 °C for 24 h. The mass of dry material was determined before and after exposure,

Ultimate tensile strength testing. Mechanical testing was performed to determine the ultimate tensile strength (UTS) by pulling hydrated 1 × 3 cm pieces at a constant rate of approximately 1 mm per second using a Chattilon ER 114/2. Results for both groups were averaged.

Disclaimer of Potential Conflicts of Interest

No potential conflicts of interest were disclosed.

Acknowledgments

The authors would like to thank Nanotherapeutics, Inc. for their continued support of this research.

References

1. Cillo JE Jr., Caloss R, Miles BA, Ellis E 3rd. An unusual response associated with cross-linked porcine dermal collagen (ENDURAGen) used for reconstruction of a post-traumatic lateral nasal wall deformity. J Oral Maxillofac Surg 2007; 65:1017-22; PMID:17448856; http://dx.doi.org/10.1016/j.joms.2005.08.024
2. Conklin BS, Richter ER, Kreutziger KL, Zhong DS, Chen C. Development and evaluation of a novel decellularized vascular xenograft. Med Eng Phys 2002; 24:173-83; PMID:12062176; http://dx.doi.org/10.1016/S1350-4533(02)00010-3
3. Dahl SL, Koh J, Prabhakar V, Niklason LE. Decellularized native and engineered arterial scaffolds for transplantation. Cell Transplant 2003; 12:659-66; PMID:14579934
4. Schmidt CE, Baier JM. Acellular vascular tissues: natural biomaterials for tissue repair and tissue engineering. Biomaterials 2000; 21:2215-31; PMID:11026628; http://dx.doi.org/10.1016/S0142-9612(00)00148-4
5. Uchimura E, Sawa Y, Taketani S, Yamanaka Y, Hara M, Matsuda H, et al. Novel method of preparing acellular cardiovascular grafts by decellularization with poly(ethylene glycol). J Biomed Mater Res A 2003; 67:834-7; PMID:14613231; http://dx.doi.org/10.1002/jbm.a.10097
6. Cartmell JS, Dunn MG. Effect of chemical treatments on tendon cellularity and mechanical properties. J Biomed Mater Res 2000; 49:134-40; PMID:10559756; http://dx.doi.org/10.1002/(SICI)1097-4636(200001)49:1<134::AID-JBM17>3.0.CO;2-D
7. Woods T, Gratzer PF. Effectiveness of three extraction techniques in the development of a decellularized bone-anterior cruciate ligament-bone graft. Biomaterials 2005; 26:7339-49; PMID:16023194; http://dx.doi.org/10.1016/j.biomaterials.2005.05.066
8. Borschel GH, Dennis RG, Kuzon WM Jr. Contractile skeletal muscle tissue-engineered on an acellular scaffold. Plast Reconstr Surg 2004; 113:595-602, discussion 603-4; PMID:14758222; http://dx.doi.org/10.1097/01.PRS.0000101064.62289.2F
9. Faleris JA, Hernandez RM, Wetzel D, Dodds R, Greenspan DC. In-vivo and in-vitro histological evaluation of two commercially available acellular dermal matrices. Hernia. 2010; PMID:21103998
10. Badylak SF, Lantz GC, Coffey A, Geddes LA. Small intestinal submucosa as a large diameter vascular graft in the dog. J Surg Res 1989; 47:74-80; PMID:2739401; http://dx.doi.org/10.1016/0022-4804(89)90050-4
11. Badylak SF, Tullius R, Kokini K, Shelbourne KD, Klootwyk T, Voytik SL, et al. The use of xenogeneic small intestinal submucosa as a biomaterial for Achilles tendon repair in a dog model. J Biomed Mater Res 1995; 29:977-85; PMID:7593041; http://dx.doi.org/10.1002/jbm.820290809
12. Kropp BP, Eppley BL, Prevel CD, Rippy MK, Harruff RC, Badylak SF, et al. Experimental assessment of small intestinal submucosa as a bladder wall substitute. Urology 1995; 46:396-400; PMID:7660517; http://dx.doi.org/10.1016/S0090-4295(99)80227-1
13. Chen F, Yoo JJ, Atala A. Acellular collagen matrix as a possible "off the shelf" biomaterial for urethral repair. Urology 1999; 54:407-10; PMID:10475343; http://dx.doi.org/10.1016/S0090-4295(99)00179-X
14. Freytes DO, Badylak SF, Webster TJ, Geddes LA, Rundell AE. Biaxial strength of multilaminated extracellular matrix scaffolds. Biomaterials 2004; 25:2353-61; PMID:14741600; http://dx.doi.org/10.1016/j.biomaterials.2003.09.015
15. Gilbert TW, Stolz DB, Biancaniello F, Simmons-Byrd A, Badylak SF. Production and characterization of ECM powder: implications for tissue engineering applications. Biomaterials 2005; 26:1431-5; PMID:15482831; http://dx.doi.org/10.1016/j.biomaterials.2004.04.042
16. Metcalfe AD, Ferguson MW. Tissue engineering of replacement skin: the crossroads of biomaterials, wound healing, embryonic development, stem cells and regeneration. J R Soc Interface 2007; 4:413-37; PMID:17251138; http://dx.doi.org/10.1098/rsif.2006.0179
17. Hiles M, Record Ritchie RD, Altizer AM. Are biologic grafts effective for hernia repair?: a systematic review of the literature. Surg Innov 2009; 16:26-37; PMID:19223383; http://dx.doi.org/10.1177/1553350609331397
18. Nimni ME, Cheung D, Strates B, Kodama M, Sheikh K. Chemically modified collagen: a natural biomaterial for tissue replacement. J Biomed Mater Res 1987; 21:741-71; PMID:3036880; http://dx.doi.org/10.1002/jbm.820210606
19. Pachence JM. Collagen-based devices for soft tissue repair. J Biomed Mater Res 1996; 33:35-40; PMID:8734072; http://dx.doi.org/10.1002/(SICI)1097-4636(199621)33:1<35::AID-JBM6>3.0.CO;2-N
20. Stone KR, Steadman JR, Rodkey WG, Li ST. Regeneration of meniscal cartilage with use of a collagen scaffold. Analysis of preliminary data. J Bone Joint Surg Am 1997; 79:1770-7; PMID:9409790
21. Ma L, Gao C, Mao Z, Zhou J, Shen J. Enhanced biological stability of collagen porous scaffolds by using amino acids as novel cross-linking bridges. Biomaterials 2004; 25:2997-3004; PMID:14967532; http://dx.doi.org/10.1016/j.biomaterials.2003.09.092
22. Zeeman R, Dijkstra PJ, van Wachem PB, van Luyn MJ, Hendriks M, Cahalan PT, et al. Successive epoxy and carbodiimide cross-linking of dermal sheep collagen. Biomaterials 1999; 20:921-31; PMID:10353646; http://dx.doi.org/10.1016/S0142-9612(98)00242-7
23. Khor E. Methods for the treatment of collagenous tissues for bioprostheses. Biomaterials 1997; 18:95-105; PMID:9022956; http://dx.doi.org/10.1016/S0142-9612(96)00106-8
24. Jorge-Herrero E, Fernández P, Turnay J, Olmo N, Calero P, García R, et al. Influence of different chemical cross-linking treatments on the properties of bovine pericardium and collagen. Biomaterials 1999; 20:539-45; PMID:10213357; http://dx.doi.org/10.1016/S0142-9612(98)90205-8
25. Dahm M, Lyman WD, Schwell AB, Factor SM, Frater RW. Immunogenicity of glutaraldehyde-tanned bovine pericardium. J Thorac Cardiovasc Surg 1990; 99:1082-90; PMID:2141662
26. Huma P, Bezuidenhout D, Torrianni M, Hendriks M, Zilla P. Optimization of diamine bridges in glutaraldehyde treated bioprosthetic aortic wall tissue. Biomaterials 2002; 23:2099-103; PMID:11962649; http://dx.doi.org/10.1016/S0142-9612(01)00302-7
27. Maranto AR, Schoen FJ. Alkaline phosphatase activity of glutaraldehyde-treated bovine pericardium used in bioprosthetic cardiac valves. Circ Res 1988; 63:844-8; PMID:3139323; http://dx.doi.org/10.1161/01.RES.63.4.844
28. Courtman DW, Errett BF, Wilson GJ. The role of crosslinking in modification of the immune response elicited against xenogenic vascular acellular matrices. J Biomed Mater Res 2001; 55:576-86; PMID:11288086; http://dx.doi.org/10.1002/1097-4636(20010615)55:4<576::AID-JBM1051>3.0.CO;2-9
29. Sung HW, Hsu HL, Shih CC, Lin DS. Cross-linking characteristics of biological tissues fixed with monofunctional or multifunctional epoxy compounds. Biomaterials 1996; 17:1405-10; PMID:8830967; http://dx.doi.org/10.1016/0142-9612(96)87282-6
30. Pieper JS, Oosterhof A, Dijkstra PJ, Veerkamp JH, van Kuppevelt TH. Preparation and characterization of porous crosslinked collagenous matrices containing bioavailable chondroitin sulphate. Biomaterials 1999; 20:847-58; PMID:10226711; http://dx.doi.org/10.1016/S0142-9612(98)00240-3
31. van Wachem PB, van Luyn MJ, Olde Damink LH, Dijkstra PJ, Feijen J, Nieuwenhuis P. Biocompatibility and tissue regenerating capacity of crosslinked dermal sheep collagen. J Biomed Mater Res 1994; 28:353-63; PMID:8077250; http://dx.doi.org/10.1002/jbm.820280310
32. Yannas IV. Tissue regeneration by use of collagen-glycosaminoglycan copolymers. Clin Mater 1992; 9:179-87; PMID:10149968; http://dx.doi.org/10.1016/0267-6605(92)90098-E
33. Alexander SA, Donoff RB. The glycosaminoglycans of open wounds. J Surg Res 1980; 29:422-9; PMID:7421186; http://dx.doi.org/10.1016/0022-4804(80)90055-4
34. Ruiz-Cardona L, Sanzgiri YD, Benedetti LM, Stella VJ, Topp EM. Application of benzyl hyaluronate membranes as potential wound dressings: evaluation of water vapour and gas permeabilities. Biomaterials 1996; 17:1639-43; PMID:8842370; http://dx.doi.org/10.1016/0142-9612(95)00324-X

35. Chen WY, Abatangelo G. Functions of hyaluronan in wound repair. Wound Repair Regen 1999; 7:79-89; PMID:10231509; http://dx.doi.org/10.1046/j.1524-475X.1999.00079.x
36. King SR, Hickerson WL, Proctor KG. Beneficial actions of exogenous hyaluronic acid on wound healing. Surgery 1991; 109:76-84; PMID:1984639
37. Oksala O, Salo T, Tammi R, Häkkinen L, Jalkanen M, Inki P, et al. Expression of proteoglycans and hyaluronan during wound healing. J Histochem Cytochem 1995; 43:125-35; PMID:7529785; http://dx.doi.org/10.1177/43.2.7529785
38. Tomihata K, Ikada Y. Crosslinking of hyaluronic acid with water-soluble carbodiimide. J Biomed Mater Res 1997; 37:243-51; PMID:9358318; http://dx.doi.org/10.1002/(SICI)1097-4636(199711)37:2<243::AID-JBM14>3.0.CO;2-F
39. Olde Damink LH, Dijkstra PJ, van Luyn MJ, van Wachem PB, Nieuwenhuis P, Feijen J. Cross-linking of dermal sheep collagen using a water-soluble carbodiimide. Biomaterials 1996; 17:765-73; PMID:8730960; http://dx.doi.org/10.1016/0142-9612(96)81413-X
40. Olde Damink LH, Dijkstra PJ, van Luyn MJ, van Wachem PB, Nieuwenhuis P, Feijen J. In vitro degradation of dermal sheep collagen cross-linked using a water-soluble carbodiimide. Biomaterials 1996; 17:679-84; PMID:8672629; http://dx.doi.org/10.1016/0142-9612(96)86737-8
41. Rao KP. Recent developments of collagen-based materials for medical applications and drug delivery systems. J Biomater Sci Polym Ed 1995; 7:623-45; PMID:8924427
42. Li CQ, Huang B, Luo G, Zhang CZ, Zhuang Y, Zhou Y. Construction of collagen II/hyaluronate/chondroitin-6-sulfate tri-copolymer scaffold for nucleus pulposus tissue engineering and preliminary analysis of its physico-chemical properties and biocompatibility. J Mater Sci Mater Med 2010; 21:741-51; PMID:19763796; http://dx.doi.org/10.1007/s10856-009-3871-5
43. Park SN, Lee HJ, Lee KH, Suh H. Biological characterization of EDC-crosslinked collagen-hyaluronic acid matrix in dermal tissue restoration. Biomaterials 2003; 24:1631-41; PMID:12559823; http://dx.doi.org/10.1016/S0142-9612(02)00550-1
44. Park SN, Park JC, Kim HO, Song MJ, Suh H. Characterization of porous collagen/hyaluronic acid scaffold modified by 1-ethyl-3-(3-dimethylaminopropyl)carbodiimide cross-linking. Biomaterials 2002; 23:1205-12; PMID:11791924; http://dx.doi.org/10.1016/S0142-9612(01)00235-6
45. Cao H, Xu SY. EDC/NHS-crosslinked type II collagen-chondroitin sulfate scaffold: characterization and in vitro evaluation. J Mater Sci Mater Med 2008; 19:567-75; PMID:18058201; http://dx.doi.org/10.1007/s10856-007-3281-5
46. Lee CR, Grodzinsky AJ, Spector M. The effects of cross-linking of collagen-glycosaminoglycan scaffolds on compressive stiffness, chondrocyte-mediated contraction, proliferation and biosynthesis. Biomaterials 2001; 22:3145-54; PMID:11603587; http://dx.doi.org/10.1016/S0142-9612(01)00067-9
47. Pieper JS, Hafmans T, Veerkamp JH, van Kuppevelt TH. Development of tailor-made collagen-glycosaminoglycan matrices: EDC/NHS crosslinking, and ultrastructural aspects. Biomaterials 2000; 21:581-93; PMID:10701459; http://dx.doi.org/10.1016/S0142-9612(99)00222-7
48. Moore ST, Katz JM, Zhukauskas RM, Hernandez RM, Lewis CS, Supronowicz PR, et al. Osteoconductivity and osteoinductivity of Puros(R) DBM putty. J Biomater Appl 2011; 26:151-71; PMID:20566657; http://dx.doi.org/10.1177/0885328210366061
49. Ames BN, Mccann J, Yamasaki E. Methods for detecting carcinogens and mutagens with the Salmonella/mammalian-microsome mutagenicity test. Mutat Res 1975; 31:347-64; PMID:768755; http://dx.doi.org/10.1016/0165-1161(75)90046-1